HAL
open science

Statistics of high-altitude and high-latitude O+ ion outflows observed by Cluster/CIS

S. Arvelius, M. Yamauchi, Hans Nilsson, R. Lundin, Y. Hobara, H. Rème, M.B. Bavassano-Cattaneo, G. Paschmann, A. Korth, L. M. Kistler, et al.

To cite this version:

S. Arvelius, M. Yamauchi, Hans Nilsson, R. Lundin, Y. Hobara, et al.. Statistics of high-altitude and high-latitude O+ ion outflows observed by Cluster/CIS. Annales Geophysicae, 2005, 23 (5), pp.1909-1916. hal-00329420

HAL Id: hal-00329420

https://hal.science/hal-00329420v1

Submitted on 18 Jun 2008

HAL is a multi-disciplinary open access archive for the deposit and dissemination of scientific research documents, whether they are published or not. The documents may come from teaching and research institutions in France or abroad, or from public or private research centers.

L'archive ouverte pluridisciplinaire **HAL**, est destinée au dépôt et à la diffusion de documents scientifiques de niveau recherche, publiés ou non, émanant des établissements d'enseignement et de recherche français ou étrangers, des laboratoires publics ou privés.

Annales Geophysicae, 23, 1909–1916, 2005
SRef-ID: 1432-0576/ag/2005-23-1909
© European Geosciences Union 2005

Annales Geophysicae

Statistics of high-altitude and high-latitude O^+ ion outflows observed by Cluster/CIS

S. Arvelius[1], M. Yamauchi[1], H. Nilsson[1], R. Lundin[1], Y. Hobara[1], H. Rème[2], M. B. Bavassano-Cattaneo[3], G. Paschmann[4], A. Korth[5], L. M. Kistler[6], and G. K. Parks[7]

[1]Swedish Institute of Space Physics (IRF), Box 812, 98128 Kiruna, Sweden
[2]Centre d'Etude Spatiale des Rayonnements, Toulouse, France
[3]Instituto di Fisica dello Spazio Interplanetario, Roma, Italy
[4]Max-Planck-Institut für Extraterrestrische Physik, Garching, Germany
[5]Max-Planck-Institut für Sonnensystemforschung, Katlenburg-Lindau, Germany
[6]University of New Hampshire, Durham, USA
[7]Space Science Laboratory, UC Berkeley, USA

Received: 2 March 2005 – Revised: 19 April 2005 – Accepted: 10 May 2005 – Published: 28 July 2005

Abstract. The persistent outflows of O^+ ions observed by the Cluster CIS/CODIF instrument were studied statistically in the high-altitude (from 3 up to 11 R_E) and high-latitude (from 70 to ∼90 deg invariant latitude, ILAT) polar region. The principal results are: (1) Outflowing O^+ ions with more than 1 keV are observed above 10 R_E geocentric distance and above 85 deg ILAT location; (2) at 6–8 R_E geocentric distance, the latitudinal distribution of O^+ ion outflow is consistent with velocity filter dispersion from a source equatorward and below the spacecraft (e.g. the cusp/cleft); (3) however, at 8–12 R_E geocentric distance the distribution of O^+ outflows cannot be explained by velocity filter only. The results suggest that additional energization or acceleration processes for outflowing O^+ ions occur at high altitudes and high latitudes in the dayside polar region.

Keywords. Magnetospheric physics (Magnetospheric configuration and dynamics, Solar wind-magnetosphere interactions)

1 Introduction

Ionized atomic oxygen (O^+) ions of terrestrial origin are a good tracer to investigate how the Earth's ionosphere/magnetosphere responds to solar activities. By tracing them and examining their properties and distributions in the magnetosphere we can also survey the dynamical structures of the magnetosphere. The O^+ ions may also play an important role in the dynamics of the magnetosphere, in particular, during large magnetic storms (e.g. Moore et al., 1999a; Blanc et al., 1999, and references therein). Furthermore, the escape of ionospheric origin ions helps us to understand non-thermal energization and the loss of atmosphere in the field of planetary physics (e.g. Lundin et al., 2004).

The main energization/acceleration mechanisms that have been known for ionospheric O^+ are wave-particle interactions (resonance and heating), parallel potential drops, and centrifugal acceleration. At low altitudes, Norqvist et al. (1998) have reported in their statistical study that most O^+ heating and outflows were caused by ion energization associated with broad-band, low-frequency (BBLF) waves and that the major source of O^+ ion energization is located in the prenoon auroral region based on the Freja satellite observations (between 50° and 75° CGL (corrected geomagnetic latitude) and altitudes 1400∼1750 km). Another obvious acceleration mechanism is parallel potential drops. This is confirmed by mid-altitude satellites (2–3 R_E) (Lundin et al., 1995). Ho et al. (1994) have reported that the increase of O^+ outflow velocity below 5 R_E can be explained in part by the centrifugal acceleration (Cladis, 1986; Horwitz et al., 1994). However, it is not clear yet whether heating by waves and acceleration by parallel potential drop at low/middle altitudes are sufficient for keV oxygen in the high-altitude region. Seki et al. (2002) discussed additional energization and different paths of outflowing O^+ ions as candidates for the O^+ supply (or cold O^+ beams, COBs) in the long-distance tail/lobe utilizing both Geotail and FAST data. They suggest that cold upflowing O^+ ions are further energized up to ∼2.7 keV at high altitude, travelling over the polar region, and eventually reach the long-distance tail/lobe region. In fact, Eklund et al. (1997) have already shown the existence of keV O^+ near both sides of the high-latitude magnetopause, indicating that the keV acceleration takes place inside the polar magnetosphere.

Correspondence to: S. Arvelius
(sachiko.arvelius@irf.se)

The Cluster satellite project gives us a new and unprecedented database on this subject with mass-resolved energetic ion measurements at high altitudes (from 3 up to 11 R_E) and high latitudes (from 70 to 90 deg ILAT). Nilsson et al. (2004) recently indicated that the high altitude polar cap magnetosphere (6–12 R_E geocentric distance) is not just a passive transport region, and that a significant energization at high altitude was a likely explanation for the reported measurements. In their argument the increase in the O^+ energy toward the higher latitudes/altitudes cannot be explained only by the velocity filter effect (see Fig. 1 and refer to, e.g. Horwitz et al., 1994, concerning the velocity filter effect). We further investigate this problem in this paper.

Another item to be examined is the dependence on the geomagnetic activities. The flux of ionospheric outflow is affected by the solar condition, i.e. it increases as solar EUV flux ($F_{10.7}$) increases (Yau and André , 1997). Norqvist et al. (1998) also showed that O^+ ion outflows are strongly K_p dependent (see also Yau and André , 1997). Recently, Cully et al. (2003) have reported correlations between the O^+ ion outflow rate (energy range from <1 to 70 eV) and the solar radio flux ($F_{10.7}$), geomagnetic activity (K_p) and solar wind parameters.

There are two scientific issues that require further studies: (1) statistical evidence of high-altitude acceleration of outflowing O^+ ions, and (2) the high altitude ion outflow during different magnetospheric conditions. For (1) we investigate the energy of maximum number flux (more precisely, maximum differential particle flux) as functions of altitude and latitude. For (2) the K_p dependence on O^+ ion outflow in the high-altitude and high-latitude needs to be investigated and compared with previous works, as mentioned above.

2 Data description

The orbit and instrumentation of the Cluster satellites enable us to investigate the statistical characteristics of the O^+ ion outflow in the high-altitude and high-latitude polar region. The CIS/CODIF instrument on board the Cluster satellites is capable of identifying field-aligned upgoing O^+ ions with good pitch-angle resolution (e.g. Rème et al., 2001).

An example of polar outflowing O^+ ions is shown in Fig. 1. This data was collected during a storm period (K_p index was 6 between 06:00–09:00 UT, and 5 between 09:00–12:00 UT). According to the ACE/MAG data, the interplanetary magnetic field (IMF) B_y (in GSM coordinate) was almost constantly −20 nT during the period from 06:00 to 11:00 UT, and the IMF $B_{z,gsm}$ turned suddenly southward (from ∼+5 nT to −5 nT) at around 08:48 UT when a sharp energy enhancement of O^+ ions was observed incidentally. The Cluster satellites traversed over the polar region and presumably entered the poleward cusp or the mantle at around 09:00 UT, then crossed the magnetopause at around 10:10 UT. Figure 1 shows clearly a narrow energy band of O^+ ions between 07:00–10:00 UT, with a clearly different energy distribution compared to that of H^+ ions observed simultaneously (e.g. regarding energy of maximum number flux, H^+:60 eV and O^+:96 eV at 08:16:00 UT, and H^+:410 eV and O^+:1.7 keV at 09:30:06 UT, where $\Delta E/E$ of the CIS/CODIF is 0.16). The pitch angle time spectrogram (PAD) panel shows that O^+ ions are mostly field-aligned and upgoing. Sample velocity distributions of polar outflowing O^+ ions are shown in Fig. 2, and the velocity distributions correspond to a 4-spin (16 s) accumulation at around 08:16 UT (6.75 R_E geocentric distance), 08:42 UT (7.25 R_E) and 09:30 UT (8.13 R_E) in Fig. 1. The $V_\parallel$-$V_\perp$ distribution shows an almost field-aligned motion (drifted perpendicular to the magnetic field with a velocity of 30–50 km/s during this period) of O^+ ions. The convection ($\boldsymbol{E}\times\boldsymbol{B}$ drift) velocities of O^+ ions across the magnetic field calculated on the basis of two different instruments (CIS and EDI) on board the Cluster S/C-3 are consistent with each other (not shown). In our statistical study, we use differential particle flux because this is a robust and basic measurement of the instrument and it is possible to avoid, for example, effects of cross-talk between the H^+ and O^+ channels which may affect moment calculations in the presence of very intense H^+ fluxes, such as in the cusp. We first survey maximum differential particle flux (hereafter *MDPF*) as a function of energy for several orbits, i.e. what the distribution function of the source of O^+ ion outflow looks like on the basis of

$$J(W,\alpha,\boldsymbol{x})=\frac{\boldsymbol{v}^2}{\mathrm{m}}\mathrm{f}(\mathrm{v}_\parallel,\boldsymbol{v}_\perp,\alpha,\boldsymbol{x}), \tag{1}$$

where J is a differential particle flux, f a distribution function (or phase space density), W the energy ($=mv^2/2$), and α the solid angle. We also look at the total number density (hereafter N) as a supplementary variable to *MDPF* due to the relation; $J=N\cdot v$.

In our statistical study, we first identified by sight these beam-like outflowing O^+ ions in the 129 Cluster traversals of the polar cap and cusp (years 2001−2003 and January to May), and then calculated variables, such as energy of maximum differential particle flux (hereafter, PE), maximum differential particle flux (*MDPF*) and total number density (N), of O^+ ions during every 16 s, corresponding to the CODIF low time-resolution mode. For example, Fig. 1 contains 670 observation points plotted against location in the right side panels (with "+" marks). In this way we have a total of more than eighty thousand points. These values were compared to geomagnetic activity at different altitudes (or geocentric distances in R_E) and invariant latitudes (ILAT).

3 Result

We first examine the spatial distribution of dayside O^+ outflow events for different energies. To have enough statistics (since we have only 129 traversals), we classify the energy of the maximum number flux (PE) into 4 categories: (1)$10\leq PE<100$ eV, (2) $0.1\leq PE<1.0$ keV, (3)$1.0\leq PE<10$ keV and (4) $PE\geq 10$ keV. We then look at the occurrence rates of the different PE levels in

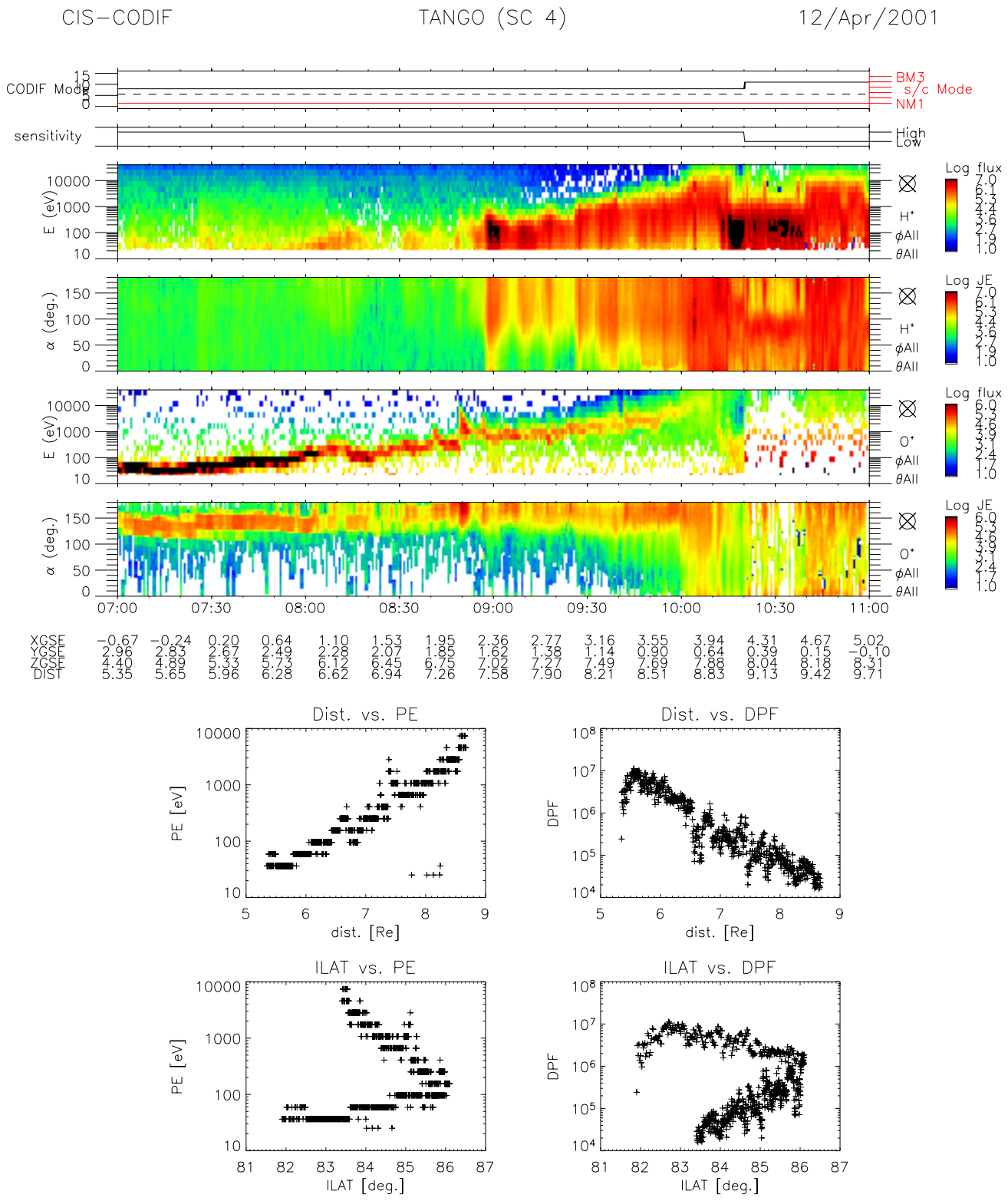

Fig. 1. Sample data on 12 April 2001. Upper panel: There are 6 panels and the first two panels from the top are detection mode and sensitivity of the CIS/CODIF instrument. Regarding the 3rd−6th panel from the top, time-energy spectrogram of H^+ given by flux (part/(cm^2·s·sr·keV)), time-pitch angle distributions (PADs) of H^+ given by energy flux, JE (keV/(cm^2·s·sr·keV)), and time-energy spectrogram and time-PADs of O^+. The observation time interval of field-aligned upgoing (or outflowing) O^+ ions is selected between 07:00 and 10:00 UT. (Bottom panel) The energy (eV) of maximum differential particle flux (abbreviated to *PE* hereafter) and the maximum differential particle flux (*MDPF* (part/(cm^2·s·sr·keV))) of field-aligned upgoing O^+ (12 April 2001, 07:00–10:00 UT) as functions of geocentric distance and invariant latitude (ILAT).

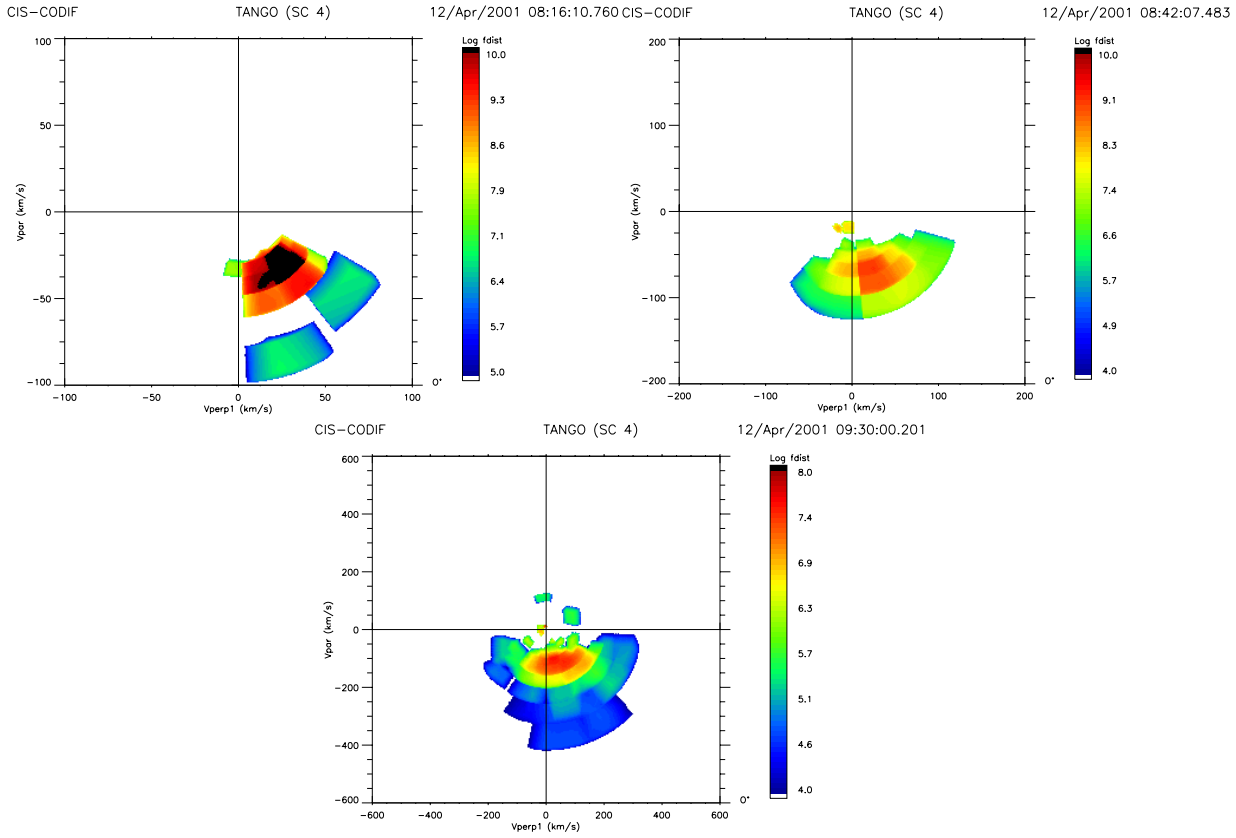

Fig. 2. Sample velocity distributions on 12 April 2001. The figures show $V_{\parallel}-V_{\perp}$ distribution and 4-spin (16 s) accumulation. The negative sign in the $V_{\parallel}$ axis means upward-going along the field line and the unit of distribution is s^3/km^6. From the top-left and clockwise: at 08:16 UT (6.75 R_E geocentric distance), 08:42 UT (7.25 R_E), and 09:30 UT (8.13 R_E). As obvious in the figures, the convection velocity of O^+ ions perpendicular to the magnetic field is calculated about ∼40 km/s.

each 2 $R_E \times 5°$ lattice for 6–12 R_E geocentric distance and 75–90 deg ILAT. The occurrence rates are taken for different geomagnetic activities, i.e. they are defined as the corresponding number of data points sorted by the criterion ($K_p \leq 3$ for geomagnetic "quiet" period and $K_p \geq 5$ for "active"), divided by the total number of data points in each 2 $R_E \times 5°$ lattice. The occurrence rates for different PE levels in different regions with regard to the dayside K_p dependence are shown in Fig. 3. We show the result only for lattices where data points exceed more than 200, to obtain good statistics in this figure. The different colours of bars represent K_p dependence, i.e. the red bar implies $K_p \leq 3$ or "quiet" and the blue bar implies $K_p \geq 5$ or "active".

Let us look at the altitudes of 7–11 R_E (8–12 R_E geocentric distance). O^+ more than 1 keV is found (more than 10%) in all the lattices at altitudes of more than 9 R_E, while those ions are found only at latitudes of less than 80 deg for the altitudes between 7 and 9 R_E (less than 5% for latitudes are more than 80 deg). We did not observe O^+ more than 1 keV at altitudes less than 7 R_E and at latitudes higher than 75 deg. Thus, accelerated O^+ at high altitudes distribute wider towards the pole than those at low altitudes. The same tendency is found for O^+ with energy 0.1–1.0 keV. This tendency is more obvious when $K_p \geq 5$ than $K_p \leq 3$, i.e. when we expect stronger poleward convections. From the K_p dependence, one may interpret this result as a sign of the velocity filter effect (Horwitz et al., 1994). Let us examine this interpretation successively below.

We first consider O^+ with energy less than 1 keV observed at 6–8 R_E geocentric distance, i.e. 5–7 R_E in altitude. Figure 3 shows that O^+ with energy more than 0.1 keV is dominant at lower latitudes (75–80 deg), and that O^+ ions with energy less than 0.1 keV is dominant at higher latitudes. Under the assumption that outflowing O^+ ions have a field-aligned velocity defined by $v_{\parallel}=\sqrt{\frac{2W_{\parallel}}{m}}$, where $W_{\parallel}$ represents the parallel kinetic energy and is equivalent to PE here, O^+ ions with 500 eV and 50 eV have velocities of 77 km/s and 25 km/s, respectively. If both O^+ ions start simultaneously going up from the ionosphere, they travel 5 R_E elevation with a time difference of ∼890 s. Taking the velocity filter effect into account with the ionospheric convection empirically ≤.01°/s, lower energy (50 eV) O^+ ions are convected about 9° poleward. This agrees with the data shown in Fig. 3.

We next consider the source of O^+ with energies of 1.0–10 keV at 10–12 R_E and 85–90 deg or the destination of

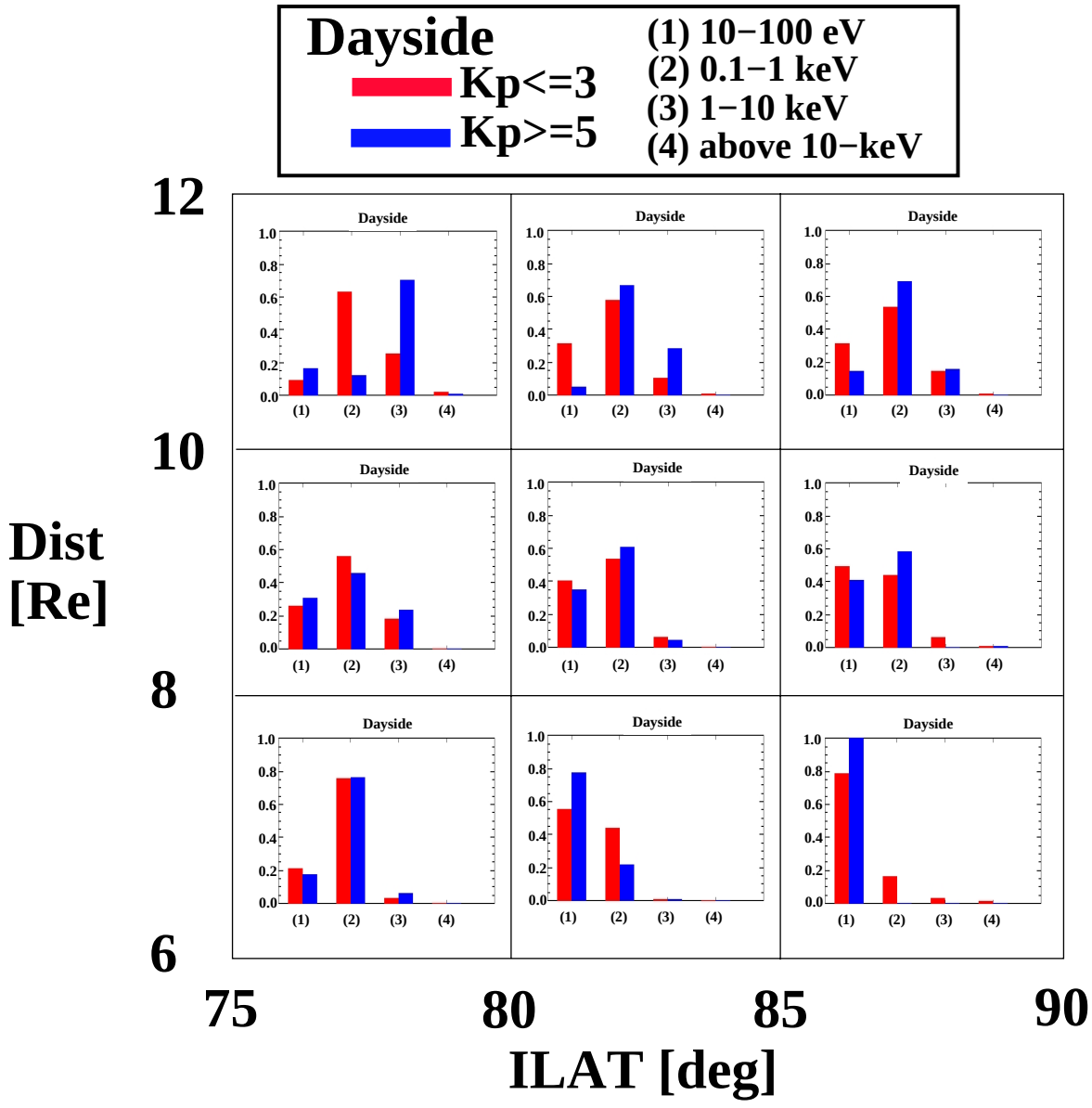

Fig. 3. The occurrence rates of different PE levels in the dayside region showing in each $2\,R_E \times 5°$ lattice. The pairs of bars are separated regarding the different PE levels in the horizontal axis (from the left, (1) $10 \leq PE < 100$ eV, (2) $0.1 \leq PE < 1$ keV, (3) $1.0 \leq PE < 10$ keV, and (4) 10 keV$\leq PE$) and the colour of bar implies "Quiet" in red and "Active" in blue, according to the K_p index. The definition of Quiet/Active is $K_p \leq 3 / K_p \geq 5$.

O^+ with energies of 1.0–10 keV at 8–10 R_E and 75–80 deg. If we use the convection velocity ∼40 km/s in the case of 12 April 2001 (∼40 km/s on averaged between 09:00–10:00 UT), during this 1-keV O^+ goes up 2 R_E elevation, where the convection distance during 2 R_E elevation is estimated as

$$2\,R_E \times \frac{40\,\mathrm{km/s}}{110\,\mathrm{km/s}} = 0.73\,R_E. \quad (2)$$

O^+ with energy of 1 keV has a velocity of ∼110 km/s under the same assumption above. This distance is nearly equivalent to 4.2° in latitude at 10 R_E geocentric distance. This means that 1-keV O^+ at 75–80 deg at 8–10 R_E can hardly convect to 85–90 deg at 10–12 R_E geocentric distance.

4 Discussion

The above result indicates that O^+ ions are eventually accelerated from less than 1 keV to more than 1 keV between 8 and 12 R_E geocentric distance. Our result agrees with the indication by Nilsson et al. (2004). The question is then what kind of mechanism causes the acceleration of O^+ at altitudes above 7 R_E. Obvious candidates from

low-/mid-altitude studies are parallel electric field (potential drops), wave-particle interaction and centrifugal acceleration. In this section we assess the possible contributions from these three candidates.

4.1 Centrifugal acceleration

Horwitz et al. (1994) showed that bulk acceleration of parallel ion outflow agrees with the centrifugal force of magnetic field curvature below 5 R_E. The centrifugal acceleration is given as

$$\left(\frac{d\mathbf{V}}{dt}\right)_{\parallel} = V_{E\times B}\frac{d\mathbf{b}}{dt} = V_{E\times B}\left(\frac{\partial \mathbf{b}}{\partial t} + \mathbf{V}_{\parallel}\cdot \nabla_{\parallel}\,\mathbf{b}\right), \quad (3)$$

where $V_{\boldsymbol{E}\times\boldsymbol{B}}$ is the $\boldsymbol{E}\times\boldsymbol{B}$ drift velocity (scalar), and $\mathbf{b}$ is the unit vector of geomagnetic field ($\mathbf{B}/|\mathbf{B}|$). The centrifugal acceleration is expected to be very efficient poleward of the cusp because of the bending direction of the geomagnetic field. For the sample event (shown in Fig. 1), the field lines are not straight, but curved. The region of interest is quite close to both the cusp and the magnetopause, which implies that the field lines are significantly bent. During the time interval from 09:00 to 10:00 UT (about 7.5 to 8.5 R_E geocentric distance), the magnetic field, B, rotates by 45 deg (not shown), and the drift velocity increases gradually. Ignoring the smaller first term of the right-hand side of Eq. 3 and assuming a constant drift velocity (40 km/s at around 09:30 UT), the acceleration is estimated roughly

$$\left(\frac{d\mathbf{V}}{dt}\right)_{\parallel} = 40\,[\mathrm{km/s}]\cdot V_{\parallel}\cdot\frac{\pi/4}{6371\,[\mathrm{km}]}\left(\frac{d\mathbf{V}}{dt}\right)_{\parallel} = 5\times10^{-3}[/\mathrm{s}]\cdot V_{\parallel}$$
$$V_{\parallel} = V_0 exp(5\times10^{-3}\cdot t[\mathrm{s}]). \quad (4)$$

Let us take O^+ of 600 eV (87 km/s) at 7.5 R_E geocentric distance (see Dist. vs. PE, upper middle panel in Fig. 1), with a 45 deg pitch angle. The acceleration value given in Eq. 4 means that for 1 R_E travel of upward going O^+,

$$\int_0^{t'} exp(5\times10^{-3}\cdot t[\mathrm{s}])dt = elevation\ \ distance/initial\ \ velocity$$
$$= 6371\,\mathrm{km}/(87\,\mathrm{km/s}). \quad (5)$$

This gives us a travel time of 73 s with the final velocity of 125 km/s (1.2 keV). While this is not enough acceleration to account for the data, which goes to about 3 keV (190 km/s), it is not negligible. However, the centrifugal acceleration is less likely to be the major contribution to the present case because of the following reason. If the centrifugal acceleration is the main contributer, we should observe energization exclusively in the parallel direction to the magnetic field, because this mechanism converts the perpendicular energy to parallel energy (e.g. Russell et al., 1999). What we observed in Fig. 2 is an energization in both perpendicular and parallel directions to the magnetic field, which contradicts what centrifugal acceleration predicts. We should also note that in our previous report (Nilsson et al., 2004), the parallel to perpendicular temperature ratio of O^+ was isotropic at altitudes between 4 to 8 R_E.

4.2 Parallel electric fields

Parallel electric field acceleration is well known to produce an upward ion beam over the aurora. However, such a parallel acceleration is generally weak over the polar cap (e.g. Eliasson et al., 1996). Another problem is the energy. Nilsson et al. (2004) showed that the O^+ field-aligned velocity is approximately equal to that of H^+ when the latter is calculated for outflowing ions only. The parallel electric field accelerates both H^+ and O^+ to the same energy instead of the same velocity. It is less likely that the acceleration is caused by field-aligned potential drop.

4.3 Wave-particle interaction

It is well known that low-frequency waves energize O^+ ions up to several hundred eV below 2000 km (Norqvist et al., 1998). Resonant wave heating/energization (see, e.g. André and Yau, 1997, for a review) may increase the perpendicular energy of ions, and the magnetic mirror force subsequently fold the ion distribution to become more beam-like at high altitudes.

If the combination of transversal heating and the magnetic mirror force is the main mechanism responsible for the observed keV ion beam, both the wave activity and the source of the wave activity must be identified. Unfortunately, there are no systematic studies of low-frequency waves in the region we are looking at. Recently, Hobara et al. (2005) reported, using Cluster EFW data, examples including the same event as Fig. 1. They saw very little wave activity in the low-altitude region (up to ~7.3 R_E), while rather strong wave activity (>1 mV/m) was observed around the ~7.6 R_E region at low frequency range, including local oxygen cyclotron frequency.

A general form of parallel acceleration by the combination of the magnetic mirror force and transversal heating by a wave is formulated in the framework of ponderomotive force (magnetic moment pumping) (e.g. Lundin and Hultqvist, 1989; Guglielmi and Lundin, 2001). Let us estimate the maximum resonant perpendicular energy. The energy gain $\Delta\epsilon$ from this resonant interaction is

$$\Delta\epsilon \simeq \frac{2}{\pi} q E v_{\perp,th}\Delta t, \quad (6)$$

where E is the amplitude of the resonant wave, $v_{\perp,th}\Delta t$ is substituted for the original $l_{\perp}$ (a characteristic transverse size of the wave field), $v_{\perp,th}$ is the perpendicular thermal velocity and Δt is the time that an ion spends in the acceleration region. During the above period (12 April 2001, 09:00–10:00 UT), $v_{\perp,th}$ is no more than about 100 km/s (see Fig. 2), E is about 1 mV/m, and Δt is about 70 s. These values give us a maximum energy gain of about 4.5 keV. In this case, 600 eV O^+ can be accelerated up to ~5 keV, although we have many uncertainties in this estimation, for example, interaction time, Δt, and resonant wave field amplitude, E. For the wave electric field we must consider the fact that ions do not feel this electric field (1 mV/m) all the time during the elapse time. Therefore, the average amplitude of the electric

field that an ion feels was less than 1 mV/m. However, even if we assume 0.1 mV/m, the energy gain is more than 0.5 keV. These values are comparable to the contribution from centrifugal acceleration or more, and it is consistent with the observed data when the case of $E \sim 1$ mV/m. Therefore, low-frequency wave activity close to the oxygen gyrofrequency (<1 Hz) may provide some energization. However, we need systematic comparisons between the O^+ beam energy and the wave intensity before making any conclusion, because this is the region where the wave activity is generally very weak. Furthermore, we know that unusual transversal heating may take place at high altitudes where shell-like distribution of O^+ is reported (Joko et al., 2004), indicating that an unknown wave-particle interaction may exist.

4.4 Sudden impulse

Figure 1 shows a burst-like appearance of near-isotropic mantle-like protons at around 08:50 UT, repeating every 5–10 min afterwards. A sudden impulse may give nonlinear acceleration. Cladis et al. (2000) have reported a 75 km/s jump in O^+ parallel velocity in the same region, in response to a CME (coronal mass ejection) (see also Moore et al., 1999b). Such a time-dependent effect (e.g. a compression of the magnetosphere accompanied by an additional centrifugal acceleration (Cladis et al., 2000) and/or magnetic moment pumping) might account for our observation.

4.5 K_p dependence

Figure 3 also shows the K_p dependence of the dayside O^+ outflow, i.e. we found an extensive keV O^+ outflow at high altitudes mainly during high K_p. This dependence is more obvious below 85 deg than above 85 deg, which cannot be explained by the velocity filter effect only, as we discussed above. Therefore, a K_p dependence indicates that the anonymous acceleration mechanism depends on geomagnetic activity.

Recently, Bouhram et al. (2004) reported, using the Cluster perigee (3.5 to 6.5 R_E) data, that (1) O^+ ion outflows vary temporally on a time scale of a few minutes and (2) the global outflow rate is much more stable and depends on the solar wind dynamic pressure, even though the local fluxes are highly variable. Regarding the latter, this generally agrees with our result on K_p dependence because K_p is generally high during high solar wind dynamic pressure. However, their study did not cover many orbits and hence the dependence on the solar wind parameters must be statistically studied.

5 Conclusions

Cluster statistics of the O^+ outflow show that dayside keV O^+ exists in over 10% of the cases at all latitudes between 75 and 90 deg at altitudes over 9 R_E. However, dayside keV O^+ exists in less than 5% of the cases between 80 to 90 deg

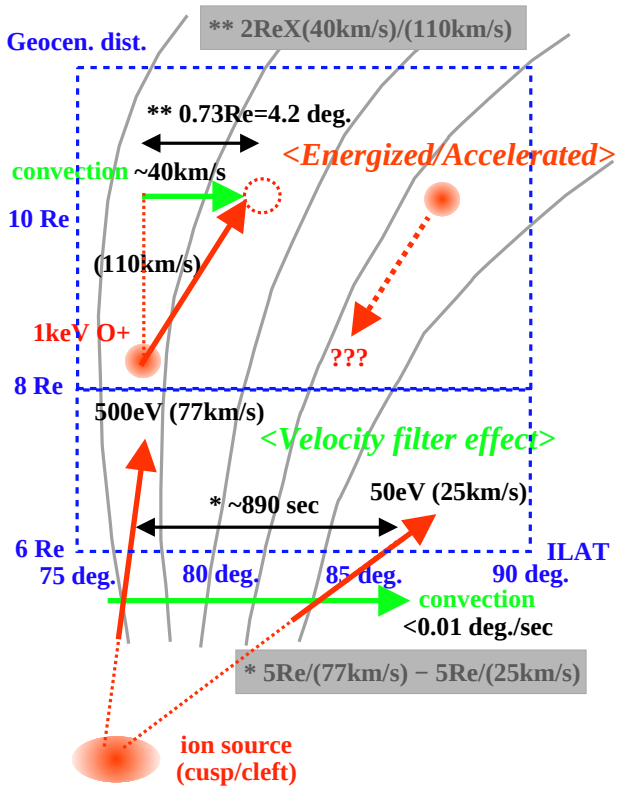

Fig. 4. The schematic (not scaled) of our conclusion. This sketch shows that we can explain outflowing O^+ ions in the polar region by the velocity filter effect below 8 R_E geocentric distance, whereas the latitudinal distribution of O^+ ions above 10 R_E cannot be explained by the velocity filter effect only. Thus, we suggest that additional energization/acceleration occurs at high altitudes and high latitudes. Note the effects by geomagnetic activity, for example, K_p dependence, are not taken into account in this sketch.

at altitudes less than 9 R_E. This result can hardly be explained by velocity filter effect alone. On the other hand, outflowing O^+ ions with energy less than 1 keV in the high-altitude and high-latitude polar region are consistent with the velocity filter effect. Hence, the continued accelerated and/or energized O^+ ions observed at high altitudes and high latitudes in the polar region imply (an) additional energization/acceleration process(es). Figure 4 shows our conclusion schematically, i.e. not exactly scaled. The strong wave activity, preferentially electromagnetic (Hobara et al., 2005) found at high altitude (>7.6 R_E), correlates well with the extra energization/acceleration, and outward acceleration is therefore a wave-particle interaction, possibly Alfvén waves causing traverse heating and parallel acceleration by ponderomotive (magnetic moment pumping) forces. However, we cannot exclude the possibility of centrifugal acceleration, especially time-dependent and associated with magnetospheric compression.

A tendency to observe keV ions at high latitude is more obvious for $K_p \geq 5$ than $K_p \leq 3$. We do not know if this K_p dependence is due to the velocity filter effect or due

to an unknown energization mechanism. To confirm the K_p dependence of O^+ outflows we are putting forward another study on (local) geomagnetic activity dependence using ASY/SYM indices. Furthermore, a study should be made of the solar wind parameters (IMF, tilt angle of IMF, dynamic pressure, and solar wind convection electric field) and their effects on the properties of outflowing O^+ (PE, $MDPF$, and N).

Acknowledgements. The CIS data and data visualization tool are provided by CNES, Toulouse, France. The K_p index is distributed by the WDC C1 for Geomagnetism at DMI, Copenhagen, Denmark (data source is the WDC C2 for Geomagnetism, Kyoto, Japan). We also thank the ACE/MAG instrument team and the ACE Science Center for providing the data. We acknowledge referees for giving us very useful comments on centrifugal acceleration.

Topical Editor T. Pulkkinen thanks C. Cully and another referee for their help in evaluating this paper.

References

André, M. and Yau, A. W.: Theories and observations of ion energization and outflow in the high latitude magnetosphere, Space Sci. Rev., 80, 27–48, 1997.

Blanc, M., Horwitz, J. L., Blake, J. B., Daglis, I., Lemaire, J. F., Moldwin,M. B., Orsini, S., Thorne, R. M., and Wolfe, R. A.: Source and Loss Processes in the Inner Magnetosphere, Chapter 4. of Magnetospheric Plasma Sources and Losses (Hultqvist, B., Øieroset, M., Paschmann, G., and Treumann, R. (Eds.)), Space Science Reviews, Vol. 88, Nos. 1–2, 1999.

Bouhram, M., Klecker, B., Paschmann, G., Rème, H., Blăgău, A., Kister,L., Puhl-Quinn, P., and Sauvaud, J.-A.: Multipoint analysis of the spatio-temporal coherence of dayside O^+ outflows with Cluster, Ann. Geophys., 22, 2507–2514, 2004, **SRef-ID: 1432-0576/ag/2004-22-2507**.

Cladis, J. B.: Parallel acceleration and transport of ions from polar ionosphere to plasma sheet, Geophys. Res. Lett., 13, 893–896, 1986.

Cladis, J. B., Collin, H. L., Lennartsson, O. W., Moore, T. E., Peterson, W. K., and Russell, C. T.: Observation of centrifugal acceleration during compression of magnetosphere, Geophys. Res. Lett., 27, 915-918, 2000.

Cully, C. M., Donovan, E. F., Yau, A. W., and Arkos, G. G.: Akebono/Suprathermal Mass Spectrometer observations of low-energy ion outflow: Dependence on magnetic activity and solar wind conditions, J. Geophys. Res., 108, 1093–1103, doi:10.1029/2002JA009587, 2003.

Eklund, U., Lundin, R., and Sandahl, I.: Measurements of O^+ in the high latitude magnetosheath, Phys. Chem. Earth., 22, 639–644, 1997.

Eliasson, L., André, M., Lundin, R., Pottelette, R., Marklund, G., and Holmgren, G.: Observations of electron conics by the Viking satellite, J. Geophys. Res., **101**, 13 225–13 238, 1996.

Guglielmi, A. and Lundin, R.: Ponderomotive upward acceleration of ions by ion cyclotron and Alfvén waves over the polar regions, J. Geophys. Res., 106, 13 219–13 236, 2001.

Ho, C. W., Horwitz, J. L., and Moore, T. E.: DE1 observation of polar O^+ stream bulk parameters and comparison with a model of the centrifugally-accelerated polar wind, Geophys. Res. Lett., 21, 2459–2462, 1994.

Hobara, Y., Nilsson, H., Arvelius, S., Lundin, R., Sundkvist, D., André, M., Cornilleau-Wehrlin, N., et al.: Cluster observation of high altitude oxygen outflow burst and associated wave activities, EGU General Assembly (abstract), 2005.

Horwitz, J. L., Ho, C. W., Scarbro, H. D., Wilson, G. R., and Moore, T. E.: Centrifugal acceleration of the polar wind, J. Geophys. Res., 99, 15 051–15 064, 1994.

Joko, S., Nilsson, H., Lundin, R., Popielwaska, B., Rème, H., Bavassano-Cattaneo, M., Paschmann, G., Korth, A., Kistler, L., and Parks, G.: Shell-like configuration in O^+ ion velocity distribution at high altitudes in the dayside magnetosphere observed by CIS/Cluster, Ann. Geophys., 22, 2473–2483, 2004, **SRef-ID: 1432-0576/ag/2004-22-2473**.

Lundin, R. and Hultqvist, B.: Ionospheric plasma escape by high-altitude electric fields: Magnetic moment "pumping", J. Geophys. Res., 94, 6665–6680, 1989.

Lundin, R., Woch, J., Yamauchi, M., and Marklund, G.: Boundary layer polarization and voltage in the 14MLT region, J. Geophys. Res., 100, 7587–7597, 1995.

Lundin, R., Barabash, S., Andersson, H., Holmström, M., Grigoriev, A., Yamauchi, M., et al.: Solar Wind-Induced Atmospheric Erosion at Mars: First Results from ASPERA-3 on Mars Express, Science, 305, 24 September 2004.

Moore, T. E., Lundin, R., Alcayde, D., André, M., Ganguli, S. B., Temerin, M., Yau, A.: Source Processes in the High-Latitude Ionosphere, Chapter 2. of Magnetospheric Plasma Sources and Losses (Bengt Hultqvist, Marit Øieroset, Goetz Paschmann and Rudolf Treumann (Eds.)), Space Science Reviews, Vol. 88, 1–2, 1999a.

Moore, T. E., Peterson, W. K., Russell, C. T., Chandler, M. O., Collier, M. R., Collin, H. L., Craven, P. D., Fitzenreiter, R., Giles, B. L., and Pollock, C. J.: Ionospheric mass ejection in response to a coronal mass ejection, Geophys. Res. Lett., 26, 2339–2342, 1999b.

Nilsson, H., Joko, S., Lundin, R., Rème, H., Sauvaud, J.-A., Dandouras, I., Balogh, A., Carr, C., Kistler, L. M., Klecker, B., Carlson, C. W., Bavassano-Cattaneo, M. B., Korth, A.: The structure of high altitude O+ energization and outflow: a case study, Ann. Geophys., 22, 2497–2506, 2004, **SRef-ID: 1432-0576/ag/2004-22-2497**.

Norqvist, P., André, M., and Tryland, M.: A statistical study of ion energization mechanisms in the auroral region, J. Geophys. Res., 103, 23459–23474, 1998.

Rème, H., Aoustin, C., Bosqued, J. M., et al.: First multispacecraft ion measurements in and near the Earth's magnetosphere with the identical Cluster ion spectrometry (CIS) experiment, Ann. Geophys., 19, 1303–1354, 2001, **SRef-ID: 1432-0576/ag/2001-19-1303**.

Russell, C. T., Zhou, X. W., Chi, P. J., Kawano, H., Moore, T. E., Peterson,W. K., Cladis, J. B. and Singer, H. J.: Sudden Compression of the outer Magnetosphere associated with an ionospheric mass ejection, Geophys. Res. Lett., 26, 2343–2346, 1999.

Seki, K., Elphic, R. C., Thomsen, M. F., Bonnell, J., McFadden, J. P., Lund,E. J., Hirahara, M., Terasawa, T., and Mukai, T.: A new perspective on plasma supply mechanisms to the magnetotail from a statistical comparison of dayside mirroring O^+ at low altitudes with lobe/mantle beams, J. Geophys. Res., 107, 1047–1058, doi.10.1029/2001JA900122, 2002.

Yau, A. W. and André, M.: Sources of ion outflow in the high latitude ionosphere, Space Sci. Rev., 80, 1–25, 1997.